

## On triaxial ellipsoidal quantum dots

This article has been downloaded from IOPscience. Please scroll down to see the full text article.

2004 J. Phys.: Condens. Matter 16 1087

(<http://iopscience.iop.org/0953-8984/16/7/008>)

View [the table of contents for this issue](#), or go to the [journal homepage](#) for more

Download details:

IP Address: 129.252.86.83

The article was downloaded on 27/05/2010 at 12:44

Please note that [terms and conditions apply](#).

# On triaxial ellipsoidal quantum dots

L C Lew Yan Voon<sup>1</sup> and M Willatzen

Mads Clausen Institute, University of Southern Denmark, Grundtvigs Allé 150,  
DK-6400 Sønderborg, Denmark

E-mail: llew@wpi.edu

Received 20 October 2003

Published 6 February 2004

Online at [stacks.iop.org/JPhysCM/16/1087](http://stacks.iop.org/JPhysCM/16/1087) (DOI: 10.1088/0953-8984/16/7/008)

## Abstract

The bound-state problem for triaxial ellipsoidal infinite-barrier quantum dots has been solved. It is exactly solvable in terms of ellipsoidal coordinates and the eigenmodes are written in terms of Lamé wavefunctions. The need for all eight types of functions is shown. This presents a generalization over previous work on spheres and spheroids. Splitting of degeneracy and level crossing are obtained.

(Some figures in this article are in colour only in the electronic version)

## 1. Introduction

Semiconductor quantum dots (QDs) are excellent model systems of quantum mechanics since they can be grown in a variety of shapes and sizes [1–3], including as QD molecules [4]. In particular, a very good mathematical model of the electron states in many of the structures (the materials must have large bandgap materials and sizes of at least tens of ångströms) is a one-band Schrödinger equation with an effective mass replacing the free-electron mass and an infinite potential barrier outside the dot (for colloidal QDs). Such a model study is extremely useful since it is often exactly solvable, thereby providing a physical insight into the problem and a limiting case that more complicated models must reduce to. As one example, such a model allowed the discovery of a critical radius for modulated nanowires [5], a result later confirmed in a multiband calculation. Furthermore, similar mathematical equations arise in other areas of physics such as electromagnetism and acoustics.

A wide variety of shapes have been made and theoretically studied over the years. Examples are rectangular boxes [3, 6, 7], discs or cylinders [8], spheres [9], cones [10], spheroids [11, 12], parabolic lenses [13, 14] and parabolic cylinders [15]. Of these, the spherical shape is probably the most popular since simple chemical growth techniques (e.g. colloidal growth) produce spherical nanocrystals. It is obvious that realistic QDs might not be perfect

<sup>1</sup> Permanent address: Department of Physics, Worcester Polytechnic Institute, 100 Institute Road, Worcester, MA 01609, USA.

spheres and this has led to the theoretical study of spheroidal QDs. However, previous works have often referred to these QDs as ellipsoids (e.g. [12]); strictly speaking, they are only ellipsoids of revolution. Nevertheless, it is known that the triaxial ellipsoid problem can also be solved exactly [16] in the sense that the partial differential equation can be separated in terms of ellipsoidal coordinates (EC). Mathematically, the problem is one of solving Helmholtz's equation with Dirichlet boundary conditions and this problem is known to be separable in 11 coordinate systems [16]. What makes the solution in EC even more important (apart from the fact that it does not appear to have been solved yet) is the fact that the other ten coordinate systems can be considered as degenerate forms of the former. In this paper, we solve Schrödinger's equation in ellipsoidal coordinates and compute the bound states for ellipsoidal QDs.

## 2. Schrödinger's equation in ellipsoidal coordinates

The ellipsoidal coordinates  $\xi_1, \xi_2, \xi_3$  are defined in terms of the Cartesian ones as follows [16–18]:

$$\begin{aligned} x &= \frac{(\xi_1^2 - a^2)^{1/2}(\xi_2^2 - a^2)^{1/2}(\xi_3^2 - a^2)^{1/2}}{a(a^2 - b^2)^{1/2}}, \\ y &= \frac{(\xi_1^2 - b^2)^{1/2}(\xi_2^2 - b^2)^{1/2}(\xi_3^2 - b^2)^{1/2}}{b(b^2 - a^2)^{1/2}}, \\ z &= \frac{\xi_1 \xi_2 \xi_3}{ab}, \end{aligned} \quad (1)$$

with

$$\xi_1 > a > \xi_2 > b > \xi_3 > 0. \quad (2)$$

One set of  $\xi_1, \xi_2, \xi_3$  corresponds to eight Cartesian points. The constant coordinate surfaces are ellipsoids (constant  $\xi_1$ ), confocal hyperboloids of one sheet (constant  $\xi_2$ ) and confocal hyperboloids of two sheets (constant  $\xi_3$ ).

Schrödinger's equation inside an ellipsoid can be written as

$$\nabla^2 \Psi + k^2 \Psi = 0, \quad (3)$$

where  $k^2 = 2m^*E/\hbar^2$ ,  $E$  is the energy and  $m^*$  is the effective mass. The problem is separable in EC. Writing

$$\Psi = X_1(\xi_1)X_2(\xi_2)X_3(\xi_3), \quad (4)$$

we have

$$\begin{aligned} &\sqrt{(\xi_1^2 - a^2)(\xi_1^2 - b^2)(\xi_2^2 - \xi_3^2)} \frac{1}{X_1} \frac{d}{d\xi_1} \left[ \sqrt{(\xi_1^2 - a^2)(\xi_1^2 - b^2)} \frac{dX_1}{d\xi_1} \right] \\ &+ \sqrt{(a^2 - \xi_2^2)(\xi_2^2 - b^2)(\xi_1^2 - \xi_3^2)} \frac{1}{X_2} \frac{d}{d\xi_2} \left[ \sqrt{(a^2 - \xi_2^2)(\xi_2^2 - b^2)} \frac{dX_2}{d\xi_2} \right] \\ &+ \sqrt{(a^2 - \xi_3^2)(b^2 - \xi_3^2)(\xi_1^2 - \xi_2^2)} \frac{1}{X_3} \frac{d}{d\xi_3} \left[ \sqrt{(a^2 - \xi_3^2)(b^2 - \xi_3^2)} \frac{dX_3}{d\xi_3} \right] \\ &+ k^2(\xi_1^2 - \xi_2^2)(\xi_2^2 - \xi_3^2)(\xi_1^2 - \xi_3^2) = 0. \end{aligned} \quad (5)$$

The three separated ordinary differential equations have the form [17]

$$(\xi_i^2 - a^2)(\xi_i^2 - b^2) \frac{d^2 X_i}{d\xi_i^2} + \xi_i [2\xi_i^2 - (a^2 + b^2)] \frac{dX_i}{d\xi_i} + [k^2 \xi_i^4 - \alpha_2 \xi_i^2 + \kappa] X_i = 0, \quad (6)$$

where  $\alpha_2$  and  $\kappa$  are the two separation constants. The latter is known as the ellipsoidal or Lamé wave equation. It is believed to be one of the most complicated second-order linear differential equations encountered in mathematical physics [19] and solving it is highly nontrivial. The equation has three regular singularities and one irregular singularity at infinity which originates from the confluence of two regular singularities, an integral solution does not appear to exist and a series solution leads to a five-term recursion relation. If we now set  $t = \xi_i^2/b^2$ ,  $X_i(\xi_i) = X(t)$ , we have

$$t(t - 1)(t - c) \frac{d^2 X}{dt^2} + \frac{1}{2}[3t^2 - 2(1 + c)t + c] \frac{dX}{dt} + (\lambda + \mu t + \gamma t^2)X = 0, \tag{7}$$

where

$$c = \frac{a^2}{b^2}, \quad \lambda = \frac{\kappa}{4b^2}, \quad \mu = -\frac{1}{4}\alpha_2, \quad \gamma = \frac{1}{4}k^2b^2. \tag{8}$$

In this form, Arscott *et al* [19] provided an algorithm for finding the characteristic curves (i.e.  $\mu$  and  $\lambda$  versus  $\gamma$ ) for one of the eight types of solutions. We have extended their algorithm to find all the eight types of solutions to the Helmholtz equation finite and smooth everywhere within an ellipsoid with the origin at the centre and intersections  $\pm x_0$ ,  $\pm y_0$  and  $\pm z_0$  with the  $x$ ,  $y$  and  $z$  axes. One starts by rewriting  $X$  in the general form [19]:

$$X(t) = t^{\rho/2}(t - 1)^{\sigma/2}(t - c)^{\tau/2}F(t), \tag{9}$$

where  $\rho$ ,  $\sigma$  and  $\tau$  are either 0 or 1, i.e. eight different types of  $X$  are possible, and  $F$  is an infinite series:

$$F(t) = \sum_{r=0}^{\infty} a_r(t - t_0)^r, \tag{10}$$

where  $t_0$  is a constant. Inserting equation (10) in (7) yields the recursion expression

$$\begin{aligned} N_r^0 a_r + [N_{r+1}^2 + N_{r+1}^1(r + 1) + N_{r+1}^0 r(r + 1)]a_{r+1} \\ + [N_{r+2}^2 + N_{r+2}^1(r + 2) + N_{r+2}^0(r + 2)(r + 1)]a_{r+2} \\ + [N_{r+3}^1(r + 3) + N_{r+3}^0(r + 3)(r + 2)]a_{r+3} \\ + N_{r+4}^0(r + 3)(r + 4)a_{r+4} = 0, \end{aligned} \tag{11}$$

with

$$\begin{aligned} N_r^0 &= \gamma, \\ N_{r+1}^0 &= 1, \\ N_{r+1}^1 &= \frac{1}{2}A_2, \\ N_{r+1}^2 &= \mu + \mu_0 + 2\gamma t_0, \\ N_{r+2}^0 &= 3t_0 - 1 - c, \\ N_{r+2}^1 &= A_2 t_0 - A_1, \\ N_{r+2}^2 &= \lambda - \lambda_0 + (\mu + \mu_0)t_0 + \gamma t_0^2, \\ N_{r+3}^0 &= (2t_0 - 1)(t_0 - c) + t_0^2 - t_0, \\ N_{r+3}^1 &= \frac{1}{2}A_2 t_0^2 - A_1 t_0 + \frac{1}{2}A_0, \\ N_{r+4}^0 &= (t_0^2 - t_0)(t_0 - c). \end{aligned} \tag{12}$$

One convergent independent solution is found by requiring that  $a_r = 0 \forall r \geq N$  using a backward–forward algorithm [20]; further details will be published elsewhere. In principle, two independent solutions exist for each coordinate  $\xi_i$ . The numerical method described

above leads to one well-behaved (finite) solution everywhere within the ellipsoid. The second independent solution is not finite everywhere within the ellipsoid and does not represent a physically allowable solution for our application. The solution of the Helmholtz equation consists of three steps. First, we determine the characteristic curves; we chose  $t_0 = 1$  always. Second, we subject the  $\xi_1$  equation to the boundary condition on the ellipsoidal surface. Third, we form the eigenfunctions for the three-dimensional problem from the product of the three Lamé wavefunctions of the same type; a proof of this important result can be found in, for example, Morse and Feshbach [16]. Since the solutions are obtained as series solutions, they are smooth and differentiable.

### 3. Calculations

We now apply the computed results to a physical problem that does not appear to have been solved yet: that of the bound states of an electron in an infinite-barrier ellipsoidal quantum dot. The basic quantities of interest in quantum mechanics are the energies and wavefunctions. The energies are related to the eigenvalues computed via

$$E = \frac{\hbar^2 k^2}{2m^*} = \frac{2\hbar^2}{m^* b^2} \gamma, \quad (13)$$

where  $b = (z_0^2 - y_0^2)^{1/2}$  and  $m^*$  is the effective electron mass. As is commonly done, we will assume the dot to be GaAs, for which  $m^* = 0.067 m_0$ . For most of the calculations, the semi-axes were chosen to be  $(x_0, y_0, z_0) = (100, 150, 200) \text{ \AA}$ .

We found all the energies to be nondegenerate. One can compare to the corresponding results for a spherical and a spheroidal dot [11, 12]. For the spherical dot, one can label the solutions by  $(n, l, m)$ , where  $(n - 1)$  is the number of radial nodes,  $l$  arises from the spherical symmetry and  $m$  labels the  $(2l + 1)$  degenerate solutions. The lowest states are known to be, in order of increasing energy,  $(1, 0, 0)$ ,  $(1, 1, 1) = (1, 1, \bar{1}) = (1, 1, 0)$ . For the spheroidal dot, the states are, at most, two-fold degenerate solutions  $(\pm|m|)$ . For the same interior volume, the ground state of a prolate spheroid is higher in energy than that of the equivalent sphere [12]. The lowered symmetry of the triaxial ellipsoid is responsible for the removal of the degeneracy in the latter case. Hence, our choice of  $n, m$  for the ellipsoid wavefunctions does not necessarily relate to the sphere and spheroid; they are chosen to reduce to the Lamé functions in the limit  $\gamma = 0$ .

In figure 1, the lowest wavefunction in one octant ( $x \geq 0, y \geq 0, z \geq 0$ ) is shown as a function of  $x, y$  in the  $z = 0$  plane (left plot),  $x, z$  in the  $y = 0$  plane (middle plot) and  $y, z$  in the  $x = 0$  plane (right plot), respectively. The energy is 31.25 meV ( $\gamma = 2.405$ ) and the indices  $n, m, \rho, \sigma, \tau$  are all 0. This state has no nodes along the three planes and peaks at the centre of the ellipsoid. It resembles the ground state of a spherical and a spheroidal dot [12]. For a sphere of the same volume, the ground-state energy is 27.06 meV. Thus, the ellipsoid ground-state energy is higher, as one would expect from quantum confinement arguments.

In figure 2, similar plots are shown for the first excited state along the two planes where it is nonvanishing. The energy is 49.27 meV ( $\gamma = 3.791$ ) and the indices  $n, m, \rho, \sigma, \tau$  are 0, 0, 1, 0, 0, respectively. It is therefore formed from a second type of Lamé wavefunction. This shows the need to calculate all eight types of Lamé wavefunctions. The wavefunction is zero in the  $z = 0$  plane but not in the  $y = 0$  and  $x = 0$  planes. It peaks at  $x = 0, z = z_0/2$  and  $z = 0, y = y_0/2$  in the  $y = 0$  and  $z = 0$  planes, respectively. This solution resembles the first excited state of the sphere in having a nodal plane. However, it is found to be nondegenerate, in contrast to the spherical and spheroidal cases (the latter for the (111) state). For example, for the sphere, this state would be three-fold degenerate. The energy of the corresponding

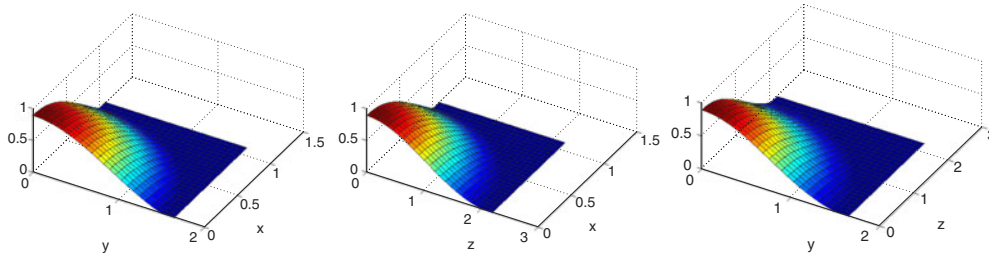


**Figure 1.** Lowest wavefunction for the ellipsoid with semi-axes  $x_0 = 1$  au,  $y_0 = 1.5$  au and  $z_0 = 2$  au (au: arbitrary units). The left, middle and right plots correspond to the  $xy$ ,  $xz$  and  $yz$  planes, respectively.

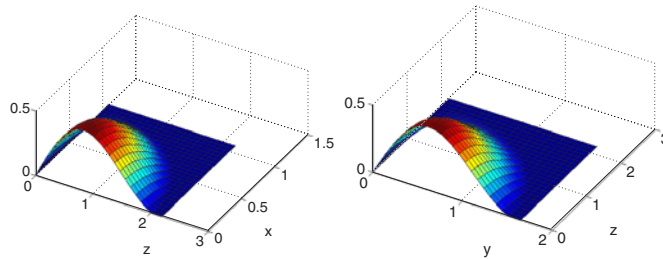


**Figure 2.** First excited state. The left (right) plot corresponds to the  $xz$  ( $yz$ ) plane. The  $z = 0$  plane is a nodal plane.

state for the sphere is 55.20 meV. This is actually higher than for the first excited state of the ellipsoid. The reason is that the splitting of the degenerate states of the sphere results in states that are below and states that are above the spherical result.

Indeed, we find that the next state (energy 58.51 meV) is equivalent to another partner of the three ( $11m$ ) states of the sphere and it vanishes in the  $y = 0$  plane. It is at a higher energy compared to the previous state because the wavefunction is oriented along the  $y$  direction, which is shorter than the  $z$  direction along which the first excited state points. For the same reason, since the semi-axis in the  $x$  direction is smaller still than in the  $y$  direction, the state corresponding to the third partner of the three ( $11m$ ) states of the sphere is even higher in energy. It turns out that it is not the fourth state but rather the sixth (energy 83.25 meV). It has, therefore, been pushed higher up in the spectrum, resulting in a level crossing with two other states (energies 72.75 and 81.51 meV). This result is due to the rather large anisotropy of the ellipsoid chosen. Indeed, our technique applies independently of the anisotropy and is, therefore, useful when perturbation methods fail [21]. The crossing effect depends upon the relative anisotropy of the ellipsoid and not on its absolute size; this can be proven from the scale invariance of the Helmholtz equation [22]. It should also occur for the spheroid but was not reported [11, 12]; it was, nevertheless, observed for an elliptical dot [23]. It is an important phenomenon that can impact the physical properties of a quantum dot [2, 24].

Finally, we briefly present a study of the shape dependence of the lowest energy state at constant volume (figure 3). We plot the  $\gamma$  parameter and the energy at constant volume for ellipsoids with different  $x_0$ ,  $z_0$  but constant  $y_0 = 1.5$  au (au stands for arbitrary units but is here chosen as 100 Å). As expected, the energy for the ellipsoid is always larger than for the corresponding sphere.

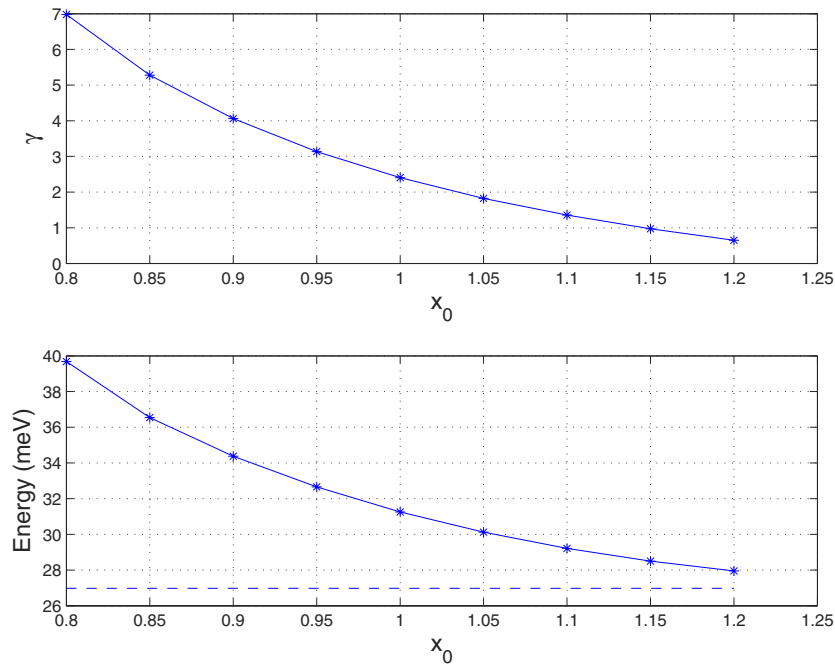


Figure 3.  $\gamma$  parameter and energy for the lowest state at constant volume for ellipsoids with different  $x_0, z_0$  but constant  $y_0 = 1.5$  au.

#### 4. Summary

In summary, we have computed the lowest bound states of a triaxial ellipsoidal quantum dot and compared them to spherical and spheroidal dots. Degeneracy splitting and level crossing, dependent upon the aspect ratio of the semi-axes of the ellipsoid but not on the absolute size, is predicted.

#### Acknowledgments

The work of LCLYV was supported by an NSF CAREER award (NSF grant no 9984059) and a Balslev award (Denmark).

#### References

- [1] Bimberg D, Grundmann M and Ledentsov N N 1999 *Quantum Dot Heterostructures* (New York: Wiley)
- [2] Hu J, Li L S, Yang W, Manna L, Wang L W and Alivisatos A P 2001 *Science* **292** 2060
- [3] Lifshitz E, Bashouti M, Kloper V, Kigel A, Eisen M S and Berger S 2003 *Nano Lett.* **3** 857
- [4] Bayer M, Hawrylak P, Hinzer K, Fafard S, Korkusinski M, Wasilewski Z R, Stern O and Forchel A 2001 *Science* **291** 451
- [5] Lew Yan Voon L C and Willatzen M 2003 *J. Appl. Phys.* **93** 9997
- [6] Schiff L I 1955 *Quantum Mechanics* (New York: McGraw-Hill)
- [7] Lew Yan Voon L C and Willatzen M 1995 *Semicond. Sci. Technol.* **10** 416
- [8] Le Goff S and Stébé B 1993 *Phys. Rev. B* **47** 1383
- [9] Éfros AI L and Éfros A L 1982 *Sov. Phys.—Semicond.* **16** 772
- [10] Lew Yan Voon L C and Willatzen M 2003 *Euro. Phys. Lett.* **62** 299
- [11] Granger S and Spence R D 1951 *Phys. Rev.* **83** 460

- [12] Cantele G, Ninno D and Iadonisi G 2000 *J. Phys.: Condens. Matter* **12** 9019
- [13] Drexler H, Leonard D, Hansen W, Kotthaus J P and Petroff P M 1994 *Phys. Rev. Lett.* **73** 2252
- [14] Lew Yan Voon L C and Willatzen M 2002 *J. Phys.: Condens. Matter* **14** 13667
- [15] Willatzen M and Lew Yan Voon L C 2003 *Physica E* **16** 286
- [16] Morse P M and Feshbach H 1953 *Methods of Theoretical Physics* (New York: McGraw-Hill)
- [17] Moon P and Spencer D E 1961 *Field Theory Handbook* (Berlin: Springer)
- [18] Arfken G B 1966 *Mathematical Methods for Physicists* (San Diego, CA: Academic)
- [19] Arscott F M, Taylor P J and Zahar R V M 1983 *Math. Comput.* **40** 367
- [20] Zhang S and Jin J 1996 *Computation of Special Functions* (New York: Wiley)
- [21] Arscott F M 1956 *Q. J. Math. (Oxford)* **7** 161
- [22] Lew Yan Voon L C and Willatzen M 2004 *Math. Comput. Simul.* at press
- [23] Lew Yan Voon L C, Galeriu G and Willatzen M 2003 *Physica E* **18** 547
- [24] Lew Yan Voon L C and Willatzen M 2003 *IEEE J. Quantum Electron.* **39** 1424